Mon. Not. R. Astron. Soc. **372,** 479–488 (2006) doi: 10.1111/j.1365-2966.2006.10895.x

Cooling of the quasi-persistent neutron star X-ray transients KS 1731−260 and MXB 1659−29

Edward M. Cackett,[1⋆] Rudy Wijnands,[2] Manuel Linares,[2] Jon M. Miller,[3] Jeroen Homan[4] and Walter H. G. Lewin[4]

[1]*School of Physics and Astronomy, University of St. Andrews, Fife KY16 9SS*
[2]*Astronomical Institute 'Anton Pannekoek', University of Amsterdam, Kruislaan 403, 1098 SJ Amsterdam, the Netherlands*
[3]*University of Michigan, Department of Astronomy, 500 Church Street, Dennison 814, Ann Arbor, MI 48105, USA*
[4]*MIT Kavli Institute for Astrophysics and Space Research, 77 Massachusetts Avenue, Cambridge, MA 02139, USA*

Accepted 2006 July 29. Received 2006 July 12; in original form 2006 May 19

ABSTRACT

We present *Chandra* and *XMM–Newton* X-ray observations that monitor the neutron star cooling of the quasi-persistent neutron star X-ray transients KS 1731−260 and MXB 1659−29 for approximately 4 yr after these sources returned to quiescence from prolonged outbursts. In both sources the outbursts were long enough to significantly heat the neutron star crust out of thermal equilibrium with the core. We analyse the X-ray spectra by fitting absorbed neutron star atmosphere models to the observations. The results of our analysis strengthen the preliminary findings of Wijnands et al. that in both sources the neutron star crust cools down very rapidly suggesting it has a high heat conductivity and that the neutron star core requires enhanced core cooling processes. Importantly, we now detect the flattening of the cooling in both sources as the crust returns to thermal equilibrium with the core. We measure the thermal equilbrium flux and temperature in both sources by fitting a curve that decays exponentially to a constant level. The cooling curves cannot be fit with just a simple exponential decay without the constant offset. We find the constant bolometric flux and effective temperature components to be $(9.2 \pm 0.9) \times 10^{-14}$ erg cm^{-2} s^{-1} and 70.0 ± 1.6 eV in KS 1731−260 and $(1.7 \pm 0.3) \times 10^{-14}$ erg cm^{-2} s^{-1} and 51.6 ± 1.4 eV in MXB 1659−29. We note that these values are dependent on the assumed distance to the sources and the column density which was tied between the observations due to the low number of photons in the latter observations. However, importantly, the shape of the cooling curves is independent of the distance assumed. In addition, we find that the crust of KS 1731−260 cools faster than that of MXB 1659−29 by a factor of ∼2, likely due to different crustal properties. This is the first time that the cooling of a neutron star crust into thermal equilibrium with the core has been observed in such detail.

Key words: accretion, accretion discs – stars: neutron – X-rays: binaries – X-rays: individual: KS 1731−260 – X-rays: individual: MXB 1659−29.

1 INTRODUCTION

Low-mass X-ray binaries consist of either a neutron star or a black hole that accretes matter from a low-mass companion star, where mass transfer occurs because the donor star overflows its Roche lobe. The soft X-ray transients form a sub-group of low-mass X-ray binaries. The vast majority of their time is spent in a quiescent state where little accretion occurs, resulting in X-ray luminosities $<10^{34}$ erg s^{-1}. However, during outbursts (which usually last weeks to months) the mass-accretion rate rises significantly, with a corresponding large increase in brightness – the typical outburst luminosity is in the range 10^{36}–10^{39} erg s^{-1} (for reviews of neutron star and black hole transients see, e.g. Campana et al. 1998a; Remillard & McClintock 2006).

The quiescent X-ray spectra of neutron star X-ray transients can generally be characterized by two components – a soft, thermal component that dominates below a few keV, and a hard power-law tail that dominates above a few keV. The power-law component is not always present and its origin is poorly understood, though in some systems it completely dominates (e.g. EXO 1745−248 in the globular cluster Terzan 5; Wijnands et al. 2005a). Several emission mechanisms have been proposed to explain the quiescent X-ray

⋆E-mail: emc14@st-andrews.ac.uk

emission, for example, residual accretion on to the neutron star magnetosphere or pulsar shock emission (e.g. Campana et al. 1998a; Menou et al. 1999; Campana & Stella 2000; Menou & McClintock 2001). However, the mechanism most often used to explain the thermal X-ray emission is that in which the emission is due to the cooling of a hot neutron star which has been heated during outburst (van Paradijs et al. 1987; Brown, Bildsten & Rutledge 1998). In the Brown et al. (1998) model, the neutron star core is heated by nuclear reactions occurring deep in the crust due to accretion during outburst, and this heat is released as thermal emission during quiescence. Thus, the temperature of the neutron star core and surface in quiescence is then set by the time-averaged mass accretion rate and the neutron star properties. Therefore, if the time-averaged accretion rate can be estimated, studying quiescent neutron star systems can give important information about the physical processes at work in the very high densities present in neutron star cores.

Some X-ray transients (the quasi-persistent transients) spend an unusually long time in outburst, with outbursts lasting years to decades rather than the more common weeks to months. For the neutron star quasi-persistent transients, during outbursts, the crust of the neutron star is heated to a point beyond thermal equilibrium with the stellar interior. Once accretion falls to quiescent levels, the crust cools thermally, emitting X-rays, until it reaches equilibrium again with the core (e.g. Rutledge et al. 2002b). Crust cooling curves allow us to probe the properties of neutron stars, such as, the kind of core cooling processes at work (which depends on the equation of state of ultradense matter) and the heat conductivity of the crust (which likely depends on the properties of the iron lattice of the crust, such as its purity). While it is expected that the crust can cool significantly between outbursts, the neutron star core should only cool significantly on much longer time-scales. X-ray observations of the two quasi-persistent neutron star X-ray transients KS 1731−260 (Wijnands et al. 2001a; Wijnands 2002; Rutledge et al. 2002b; Wijnands et al. 2002a; Wijnands 2005) and MXB 1659−29 (Wijnands et al. 2003, 2004; Wijnands 2004, 2005) have tracked the initial cooling of these neutron stars once they went into a quiescent state. In this paper, we present additional *Chandra* and *XMM–Newton* observations that further track the cooling of these two neutron stars as they return to thermal equilibrium with the core.

1.1 KS 1731−260

KS 1731−260 was first detected in outburst in 1989 August by the *Mir-Kvant* instrument and further analysis revealed that the source was also found to be active in 1988 October (Sunyaev 1989; Sunyaev 1990). As no previous telescopes had detected this source, it was classified as a soft X-ray transient and the detection of type I X-ray bursts identified the compact object as a neutron star. Since then, until early 2001, the source remained bright and was observed by many X-ray telescopes including the ART-P and SIGMA telescopes aboard *GRANAT*, *Ginga, ROSAT, RXTE, ASCA* and *BeppoSAX* (Sunyaev et al. 1990; Yamauchi & Koyama 1990; Barret et al. 1992; Smith, Morgan & Bradt 1997; Wijnands & van der Klis 1997; Barret, Motch & Predehl 1998; Muno et al. 2000; Narita, Grindlay & Barret 2001; Kuulkers et al. 2002). In early 2001, KS 1731−260 was undetected by monitoring observations by the All-Sky Monitor (ASM) on-board the *Rossi X-ray Timing Explorer* (*RXTE*) as can be seen by the ASM light curve of this source in Fig. 1 (top panel). Further pointed *RXTE* observations with the Proportional Counter Array (PCA) and the bulge scan observations of the Galactic centre region did not detect the source, with the first non-detection by

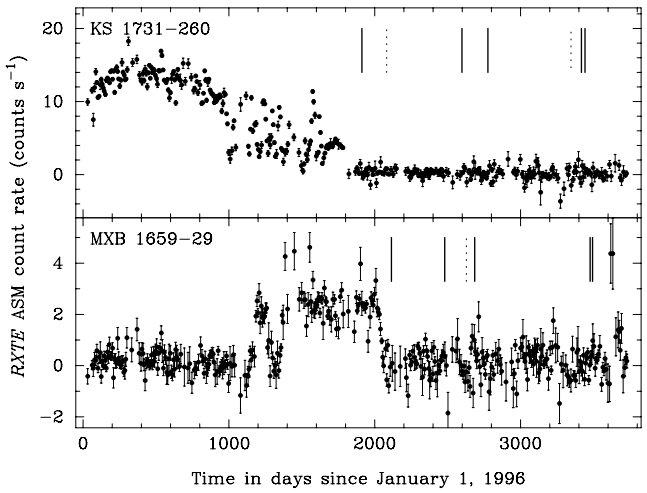

Figure 1. *RXTE* ASM 7-d averaged light curve for KS 1731−260 (top panel) and MXB 1659−29 (bottom panel). The times of the *Chandra* and *XMM–Newton* observations of these sources during quiescence are marked by solid and dotted vertical lines, respectively. The last detection of KS 1731−260 in outburst was 1847 ds after 1996 January 1, and the last detection of MXB 1659−29 was 2076 ds after 1996 January 1.

the PCA observations on 2001 February 7 (Wijnands et al. 2001a). Using archival *RXTE*/PCA data, we find that the final detection of the source with *RXTE* was on 2001 January 21, thus it was still in outburst and actively accreting on this date. We extracted the *RXTE* X-ray spectrum of the source on that day and find that a 2–10 keV unabsorbed flux of $\sim 2.3 \times 10^{-10}$ erg cm^{-2} s^{-1} which corresponds to a luminosity of $\sim 1 \times 10^{36}$ erg s^{-1} for a distance of 7 kpc (we assume a distance to KS 1731−260 of 7 kpc throughout the paper; Muno et al. 2000). Thus, KS 1731−260 went into a quiescent state sometime after 2001 January 21 and it was actively accreting for around 12.5 yr. This last detection in outburst gives a much better constraint than had previously been found for when this source turned off. Unfortunately, there are no other known outbursts of this source, thus we are unable to tell whether this is a typical outburst for this source, or whether previous outbursts have been significantly longer or shorter.

Within two months of KS 1731−260 going into a quiescent phase there was a ∼20 ks *Chandra* Advanced CCD Imaging Spectrometer (using ACIS-S mode) observation of this source on 2001 March 27 (Wijnands et al. 2001a). These authors detected the source at an unabsorbed flux of $\sim 2 \times 10^{-13}$ erg cm^{-2} s^{-1} (0.5–10 keV), which corresponds to a 0.5–10 keV luminosity of $\sim 1 \times 10^{33}$ erg s^{-1}, a factor of 10^3 lower than at the last *RXTE*/PCA detection. Observations by *BeppoSAX* confirmed the low flux of the source (Burderi et al. 2002) reported by Wijnands et al. (2001a). Wijnands et al. (2001a) note that this luminosity is much lower than expected if this is due to the cooling of the neutron star unless the source spends an unusually long amount of time in a quiescent state (at least several hundred years) and even longer if the crust is dominating emission from the neutron star, or that alternatively, enhanced cooling of the core occurs due to higher levels of neutrino emission. Rutledge et al. (2002b) note that given the long outburst, the crust would be dominating the thermal emission from the neutron star as it would have been heated significantly out of equilibrium with the core. Given the accretion history of this source Rutledge et al. (2002b) simulate the quiescent light curve for the source, finding that depending on the crust and core microphysics, the cooling time-scale for the crust to return to equilibrium with the core ranges from 1 to 30 yr.

Table 1. Details of the *Chandra* (CXO) and *XMM–Newton* (XMM) observations of KS 1731−260. The *XMM–Newton* observations 0137950201 and 0137950301 were so close in time that they were merged together. Here, we give the details for the merged data. The background-subtracted net count rate is for the 0.5–10 keV band.

ObsID (Telescope)	Date	Good time (ks)	Net count rate (counts s^{-1})
2428 (CXO)	2001 March 27	19.4	$(9.0 \pm 0.7) \times 10^{-3}$
0137950201/301 (XMM)	2001 September 13–14	46.0 (MOS1)	$(1.7 \pm 0.2) \times 10^{-3}$ (MOS1)
		46.1 (MOS2)	$(2.0 \pm 0.2) \times 10^{-3}$ (MOS2)
		33.8 (pn)	$(3.7 \pm 0.4) \times 10^{-3}$ (pn)
3796 (CXO)	2003 February 11	29.7	$(1.4 \pm 0.2) \times 10^{-3}$
3797 (CXO)	2003 August 8	29.7	$(1.1 \pm 0.2) \times 10^{-3}$
0202680101 (XMM)	2005 February 28–March 1	70.0 (MOS1)	$(2.4 \pm 1.6) \times 10^{-4}$ (MOS1)
		70.0 (MOS2)	$(6.4 \pm 1.7) \times 10^{-4}$ (MOS2)
		46.0 (pn)	$(1.1 \pm 0.4) \times 10^{-3}$ (pn)
6279 (CXO)	2005 May 10	10.4	$(0.5 \pm 0.3) \times 10^{-3}$
5468 (CXO)	2005 June 4	38.5	$(0.8 \pm 0.2) \times 10^{-3}$

Additional X-ray observations of this source in quiescence with *XMM–Newton* in 2001 September 13–14 revealed that the source had dimmed further to a 0.5–10 keV luminosity of approximately (2–5) $\times 10^{32}$ erg s^{-1} (Wijnands et al. 2002a). Under the neutron star cooling model, this decrease in luminosity is interpreted as rapid cooling of the neutron star crust (a factor of ∼2–3 in just half a year) suggesting that the crust has a high thermal conductivity and that enhanced core cooling processes are required for the core to be so cool. Preliminary analysis of two extra *Chandra* observations of this source on 2003 February 11 and 2003 August 8 yet again showed a further decrease in the luminosity of the source with a possible flattening of the luminosity cooling curve suggesting that the crust may have returned to equilibrium with the core (Wijnands 2005). In this paper, we present the final analysis of these *Chandra* data, re-analyse all the previous *Chandra* and *XMM–Newton* observations of this source in quiescence and also present two additional *Chandra* observations and one additional *XMM–Newton* observation of this source.

1.2 MXB 1659−29

MXB 1659−29 is an X-ray transient discovered by Lewin, Hoffman & Doty (1976) with *SAS-3* in 1976 October. Type-I X-ray bursts detected by these initial observations established that the compact object was a neutron star. Between 1976 October and 1978 September, this source was detected several times by both *SAS-3* and *HEAO 1* (Griffiths et al. 1978; Lewin et al. 1978; Share et al. 1978; Doxsey et al. 1979; Cominsky, Ossmann & Lewin 1983; Cominsky & Wood 1984, 1989). The source exhibits X-ray eclipses and dips with a period of ∼7.1 hr, due to the orbital period (Cominsky & Wood 1984, 1989). In 1979 July, the *Hakucho* satellite failed to detect the source (Cominsky et al. 1983), and later observations by *EXOSAT* and *ROSAT* (Oosterbroek et al. 2001; Verbunt 2001) failed to detect the source also. The 0.5–10 keV upper limit on the unabsorbed flux from the *ROSAT* observations in 1991 and 1992 is (1–2) $\times 10^{-14}$ erg cm^{-2} s^{-1} (Oosterbroek et al. 2001; Verbunt 2001; Wijnands 2002).

The source remained in a quiescent state for a period of 21 yr, until on 1999 April 2 *BeppoSAX* detected the source in outburst again (in 't Zand et al. 1999). This outburst was also detected by the *RXTE* ASM (see the ASM light curve in Fig. 1) and studied in detail by pointed observations with the *RXTE* PCA, *BeppoSAX* and *XMM–Newton* (Wachter, Smale & Bailyn 2000; Oosterbroek et al. 2001; Sidoli et al. 2001; Wijnands, Strohmayer & Franco 2001b; Wijnands et al. 2002c).

After an outburst of approximately 2.5 yr in length, MXB 1659−29 went back into a quiescent state in 2001 September. The last detection of the source was on 2001 September 7 with the *RXTE* PCA, and the source was not detected on 2001 September 14, 24, 30 (Wijnands et al. 2002c). Just over a month after the source returned to a quiescent state, *Chandra* observations, on 2001 October 15, detected it with an unabsorbed 0.5–10 keV flux of (2.7–3.6) $\times$ 10^{-13} erg cm^{-2} s^{-1} which corresponds to a 0.5–10 keV luminosity of (3.2–4.3) $\times 10^{33}$ erg s^{-1} for a distance of 10 kpc (Wijnands et al. 2003). This flux is a factor greater than 10 higher than the *ROSAT* non-detection upper limit during quiescence in the early 1990s, suggesting that the emission is dominated by thermal emission from the neutron star crust that has been heated significantly out of thermal equilibrium with the core. However, as in the case of KS 1731−260, the flux was lower than expected given the accretion history, suggesting that enhanced cooling processes are occurring in the core. Further *Chandra* observations of MXB 1659−29 in quiescence on 2002 October 15 and 2003 May 9 showed that the flux was decaying exponentially, with the source flux decreasing by a factor of 7–9 over the 1.5 yr between the 2001 and 2003 *Chandra* observations (Wijnands et al. 2004; Wijnands 2004, 2005). This is consistent with the accretion-heated crust cooling down in quiescence. The rapid time-scale of the cooling implies that the crust may have a large thermal conductivity (Wijnands et al. 2004; Wijnands 2004, 2005). In this paper, we re-analyse all the previous observations of this source in quiescence with *Chandra* and also present two additional *Chandra* observations and one additional *XMM–Newton* observation of this source.

2 OBSERVATIONS AND ANALYSIS

2.1 KS 1731−260

Here, we analyse five *Chandra* and three *XMM–Newton* observations of KS 1731−260 in a quiescent state spread over ∼4 yr since the end of the outburst in 2001 February. Details of all the observations are given in Table 1. We will first describe the analysis of the *Chandra* and then the *XMM–Newton* data.

2.1.1 Chandra analysis

All the *Chandra* observations were taken in ACIS-S configuration. The *Chandra* data were reprocessed and analysed using CIAO (v3.3)

Table 2. Neutron star atmosphere model fits to the X-ray spectrum of KS 1731−260 for five *Chandra* (CXO) and three *XMM–Newton* (XMM) observations. Luminosity is calculated assuming a distance to the source of 7 kpc. 1σ errors on the parameters are given. The MJD given corresponds to the mid-point of the observation. Note the column density parameter is tied between the observations when simultaneously fitting the data, and we determine $N_{\rm H} = (1.3 \pm 0.1) \times 10^{22}$ cm^{-2}.

ObsID (Telescope)	MJD	$kT_{\rm eff}^{\infty}$ (eV)	Bolometric flux (10^{-13} erg cm^{-2} s^{-1})	Luminosity (10^{32} erg s^{-1})
2428 (CXO)	51995.1	103^{+2}_{-3}	$4.2^{+0.3}_{-0.5}$	24^{+2}_{-3}
0137950201/301 (XMM)	52165.7	88 ± 2	2.2 ± 0.2	13 ± 1
3796 (CXO)	52681.6	76 ± 3	1.2 ± 0.2	7 ± 1
3797 (CXO)	52859.5	72 ± 4	1.0 ± 0.2	6 ± 1
0202680101 (XMM)	53430.5	70 ± 3	$0.9^{+0.2}_{-0.1}$	5 ± 1
6279 (CXO)	53500.4	67^{+6}_{-9}	0.8 ± 0.3	4 ± 2
5468 (CXO)	53525.4	70 ± 3	0.9 ± 0.2	5 ± 1

and CALDB (v3.2.1) following the standard analysis threads. For all of the *Chandra* observations, the source light curve and spectrum was extracted from a circle of radius 3 arcsec around the source position, and the background light curve and spectrum was extracted from a source-free annulus with inner radius 7 arcsec and outer radius 25 arcsec. We checked the background light curve for significant background flares, and none were found. The background-subtracted net count rates in the 0.5–10 keV band are given in Table 1.

2.1.2 XMM–Newton analysis

The first two *XMM–Newton* observations were separated by only a matter of hours, therefore we combine both of these together to increase sensitivity (as did Wijnands et al. 2002a). Here, we analyse data from the three EPIC instruments on-board *XMM–Newton* – the two metal oxide semiconductor (MOS) cameras and the pn camera which were operated in full-frame mode with the thin filter in all the observations. To analyse the *XMM–Newton* data we use the Science Analysis Software (SAS, version 6.5.0). We extract source light curves and spectra from a circle of radius 10 arcsec. The background extraction region was chosen to be a source-free circle of radius 1 arcmin close to the source position. An annulus was not used because of the location of a nearby source, 2MASSI J173 412.7–260 548, approximately 30 arcsec away. Although this source is also present in the *Chandra* data the significantly better angular resolution of *Chandra* allows the use of an annulus for background extraction.

In the merged observations (ObsID 0137950201/301) background flares were present. We kept all data where the count rate for PI $>$ 10 keV was less than 10 counts s^{-1} for both the MOS and pn. In the last *XMM–Newton* observation (ObsID 0202680101) background flares were also present. In this case, we kept all data where the count rate for PI $>$ 10 keV was less than 10 counts s^{-1} for the MOS and less than 15 counts s^{-1} for the pn. We note that in this last observation the source is not obviously present when viewing an image in the full energy range. It only becomes apparent when restricting the energy range to between 1 and 2 keV where the vast majority of the photons from the source are emitted during this observation. The net count rates for these observations are given in Table 1.

2.1.3 Spectral analysis

For spectral analysis of the data we use XSPEC (Arnaud 1996). The data were fit with an absorbed neutron star hydrogen atmosphere model (non-magnetic case; Pavlov, Shibanov & Zavlin 1991; Zavlin, Pavlov & Shibanov 1996) with the mass and radius fixed at the canonical values (1.4 $M_{\odot}$ and 10 km, respectively). Both the *Chandra* and *XMM–Newton* data were fit simultaneously with the column density tied between the observations and the temperature left as a free parameter. The column density was tied between the observations as there were too few counts in the last observations to constrain this parameter. The parameters for the EPIC MOS1, MOS2 and pn spectra for each *XMM–Newton* observation were all tied. The normalization of the neutron star atmosphere model was fixed for a distance of 7 kpc (distance determined by Muno et al. 2000). Although this distance is uncertain, if this parameter is left free it goes to an unrealistic value that would put the distance to the source at $\sim$20 kpc (although the error on the distance is very large and includes the assumed 7 kpc distance). Hence, we chose to fix the distance at 7 kpc.

The data were unbinned, due to the low number of counts in the last few observations, and the W-statistic (Wachter, Leach & Kellogg 1979) was used in the spectral fitting process with background subtraction. The W-statistic is adapted from the Cash statistic (Cash 1979), but allows background subtraction. We note that spectral fitting to the first *Chandra* observation using both χ^2 and W-statistics resulted in the same parameters to within the errors. To determine the bolometric flux we extrapolated the model to the energy range 0.01–100 keV, which gives approximate bolometric fluxes. The results of the spectral fits are detailed in Table 2. The spectral parameters for the first *Chandra* and *XMM–Newton* observations are consistent with those determined by Wijnands et al. (2002a). We also note that we get results consistent with the previously published data for KS 1731−260 Wijnands et al. (2002a) when using alternative models to the NSA model (i.e. a blackbody model).

2.1.4 Cooling curves

It is clear from Table 2 that both the effective temperature for an observer at infinity ($T_{\rm eff}^{\infty}$) and the bolometric flux $F_{\rm bol}$ decrease significantly with time. This cooling cannot be fit by a simple exponential decay, giving reduced χ^2 values of 4.3 and 4.8 for fits to the temperature and flux curves (see the dotted curves in Fig. 2). However, it is fit well by an exponential decay that levels off to a constant offset of the form $y(t) = a \exp[-(t - t_0)/b] + c$, with a a normalization constant, b the e-folding time, c a constant offset and t_0 the start time. When fitting to the data, t_0 was fixed to midday on the last day that the source was observed to be active, Modified Julian Date (MJD) 519 30.5, though we find that the other parameters

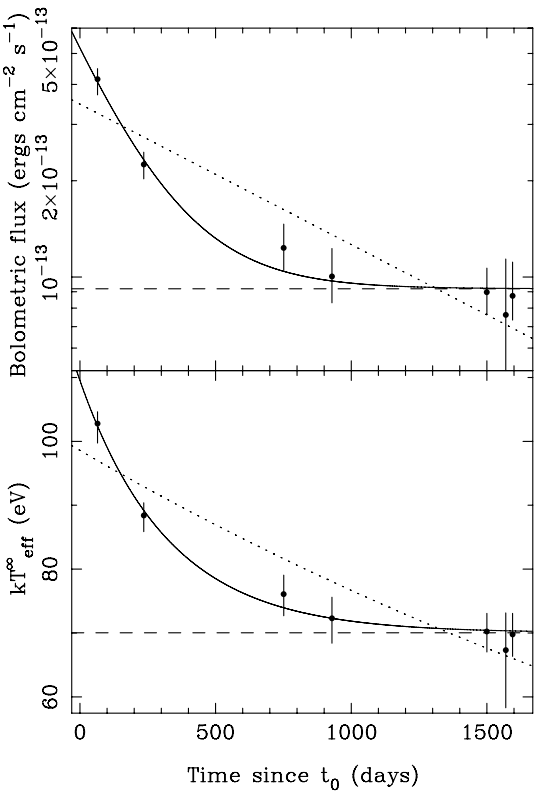

Figure 2. Cooling curves for KS1731−260. Top panel: bolometric flux versus time since t_0, the last detection of the source accreting. The solid line shows the best-fitting exponential decay to a constant. The constant is indicated as a dashed line. The dotted line shows the best-fitting simple exponential decay, which does not fit the data well. Bottom panel: effective temperature for an observer at infinity versus time since the end of the outburst. The lines are as above.

are not very sensitive to the exact value of t_0. The best-fitting cooling curves are shown in Fig. 2. For the $T^{\infty}_{\rm eff}$ curve $a = 39.5 \pm 3.6$ eV, $b = 325 \pm 101$ d and $c = 70.0 \pm 1.6$ eV, with $\chi^2_\nu = 0.2$. For the $F_{\rm bol}$ curve $a = (4.3 \pm 0.5) \times 10^{-13}$ erg cm^{-2} s^{-1}, $b = 212 \pm 60$ d and $c = (9.2 \pm 0.9) \times 10^{-14}$ erg cm^{-2} s^{-1}, with $\chi^2_\nu = 0.4$. The reason for the difference between the e-folding times of the flux and effective temperature curves is explained in Appendix A.

2.2 MXB 1659−29

We analyse five *Chandra* observations and one *XMM–Newton* observation of MXB 1659−29 whilst the source was in a quiescent state spanning a period of ∼4 yr after the end of the outburst in 2001 September. Details of the observations are given in Table 3. We will first describe the *Chandra* and then the *XMM–Newton* data reduction and analysis.

2.2.1 Chandra analysis

All the *Chandra* observations of this source were taken in the ACIS-S configuration. As in the analysis of the *Chandra* data for KS 1731−260, we reprocess and analyse the data using CIAO (v3.3), CALDB (v3.2.1) and the standard analysis threads. For all of the *Chandra* observations, the source light curve and spectrum was extracted from a circle of radius 3 arcsec around the source position, and the background light curve and spectrum was extracted from a source-free annulus with inner radius 7 arcsec and outer radius 22 arcsec. We checked the background light curve for significant background flares, and none were found.

The analysis of the data for MXB 1659−29 is complicated by the fact that this source is eclipsing with an eclipse duration of ∼900 s and period of 7.1 h (Cominsky & Wood 1984, 1989; Wachter et al. 2000; Oosterbroek et al. 2001), and so we receive no (or minimal at most) counts from the source during the eclipse in quiescence (Wijnands et al. 2003). While there are enough counts in the first *Chandra* observation to detect the eclipse in the light curve (Wijnands et al. 2003), this is impossible with later observations and so we manually reduce the exposure time by 900 s to compensate for the source being in eclipse, having checked that only one eclipse occurs during each observation using the ephemeris of Oosterbroek et al. (2001). The background-subtracted net count rates in the 0.5–10 keV band are given in Table 3.

2.2.2 XMM–Newton analysis

To analyse the *XMM–Newton* observation of MXB 1659−29 we use SAS (version 6.5.0). We analyse data from the EPIC MOS1, MOS2 and pn cameras which were operated in full-frame mode with the medium filter (the source is too faint to be detected on the RGS). The source light curve and spectrum was extracted from a circle with a 15 arcsec radius. The background light curve and spectrum was extracted from a source-free annulus with inner radius of 40 arcsec and outer radius of 100 arcsec. Several background flares were present during the observation. We chose to keep all data where the count rate for PI > 10 keV was less than 7 counts s^{-1} for the MOS and less than 10 counts s^{-1} for the pn detector. Using the ephemeris of Oosterbroek et al. (2001), we determined that three eclipses occurred during the good time of the MOS observations, and so we manually reduce the exposure times for the MOS observations by 2.7 ks. In the pn observations several flaring events occurred during the eclipse times. We determine the total amount of good

Table 3. Details of the *Chandra* (CXO) and *XMM–Newton* (XMM) observations of MXB 1659−29. The background-subtracted net count rate is for the 0.5–10 keV band.

ObsID (Telescope)	Date	Good time (ks)	Net count rate (counts s^{-1})
2688 (CXO)	2001 October 15	17.9	$(5.2 \pm 0.2) \times 10^{-2}$
3794 (CXO)	2002 October 15	26.1	$(9.8 \pm 0.6) \times 10^{-3}$
0153190101 (XMM)	2003 March 13	65.3 (MOS1)	$(3.2 \pm 0.3) \times 10^{-3}$ (MOS1)
		65.4 (MOS2)	$(2.9 \pm 0.3) \times 10^{-3}$ (MOS2)
		47.1 (pn)	$(1.1 \pm 0.1) \times 10^{-2}$ (pn)
3795 (CXO)	2003 May 9	26.2	$(3.9 \pm 0.4) \times 10^{-3}$
5469 (CXO)	2005 July 8	27.7	$(1.1 \pm 0.2) \times 10^{-3}$
6337 (CXO)	2005 July 25	17.8	$(0.7 \pm 0.2) \times 10^{-3}$

Table 4. Neutron star atmosphere model fits to the X-ray spectrum of MXB 1659−29 for five *Chandra* (CXO) and one *XMM–Newton* (XMM) observations. Luminosity is calculated assuming a distance to the source of 10 kpc. 1σ errors on the parameters are given. The MJD given correspond to the mid-point of the observation. Note the column density parameter is tied between the observations when simultaneously fitting the data, and we determine $N_{\rm H} = (0.20 \pm 0.02) \times 10^{22}$ cm^{-2}.

ObsID (Telescope)	MJD	$kT_{\rm eff}^{\infty}$ (eV)	Bolometric flux (10^{-14} erg cm^{-2} s^{-1})	Luminosity (10^{32} erg s^{-1})
2688 (CXO)	52197.8	121 ± 2	41 ± 3	49 ± 3
3794 (CXO)	52563.2	85 ± 2	10 ± 1	12 ± 1
0153190101 (XMM)	52712.2	77 ± 1	$6.6^{+0.4}_{-0.5}$	$7.9^{+0.5}_{-0.6}$
3795 (CXO)	52768.9	73^{+2}_{-1}	$5.1^{+0.6}_{-0.4}$	$6.1^{+0.7}_{-0.4}$
5469 (CXO)	53560.0	58^{+3}_{-4}	$2.0^{+0.4}_{-0.5}$	$2.4^{+0.5}_{-0.6}$
6337 (CXO)	53576.7	54^{+4}_{-5}	1.5 ± 0.5	1.8 ± 0.6

time for the pn during the eclipses to be 1.675 ks, and thus we reduce the exposure time by this amount. The net count rates for this *XMM–Newton* observation are given in Table 3.

2.2.3 Spectral analysis

We perform a similar spectral analysis for the MXB 1659−29 data as for the KS 1731−260. The *Chandra* and *XMM–Newton* spectra are left unbinned and fit simultaneously with an absorbed non-magnetic neutron star hydrogen atmosphere model using the W-statistic with background subtraction. The column density is tied between the separate observations, the mass and radius fixed at their canonical values, and the temperature was the only parameter left free between the observations. The parameters are tied between the MOS1, MOS2 and pn spectra of the *XMM–Newton* observation. The distance to this source is in the range 10–13 kpc (Muno et al. 2001; Oosterbroek et al. 2001). When leaving the normalization as a free parameter in the *Chandra* fits this leads to a distance to the source of 7.8 kpc with no constraint on the upper limit of the distance and a lower limit of 6.2 kpc. So that the uncertainty in the distance does not dominate the uncertainties in the other parameters, we fix the normalization of the neutron star atmosphere for a distance of 10 kpc. Spectral parameters determined by these fits are detailed in Table 4. The parameters we find for the first three *Chandra* observations which were previously analysed by Wijnands et al. (2004) are consistent with the values these authors determined when assuming the same distance.

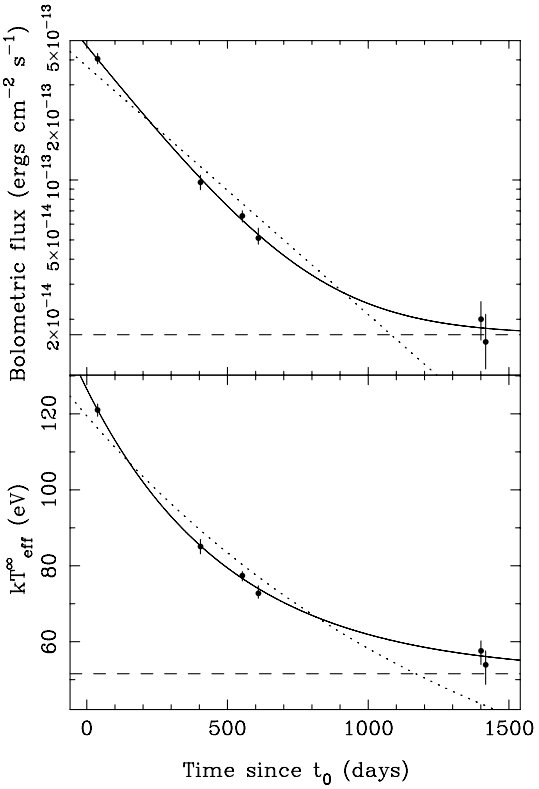

Figure 3. Cooling curves for MXB 1659−29. Top panel: bolometric flux versus time since t_0, the last detection of the source accreting. The solid line shows the best-fitting exponential decay to a constant. The constant is indicated as a dashed line. The dotted line shows the best-fitting simple exponential decay, which does not fit the data well. Bottom panel: effective temperature for an observer at infinity versus time since the end of the outburst. The lines are as above.

2.2.4 Cooling curves

From the spectral fitting we find that both $T_{\rm eff}^{\infty}$ and $F_{\rm bol}$ decrease significantly with time after the end of the outburst. We measure an unabsorbed 0.5–10 keV flux of $6.3^{+2.7}_{-2.5} \times 10^{-15}$ erg cm^{-2} s^{-1} during the last *Chandra* observation which is now lower than the upper limit from the previous non-detection with *ROSAT* in the early 1990s when the source had been in quiescence for over 10 yr. As with KS 1731−260 this cooling cannot be fit by a simple exponential decay curve, giving reduced χ^2 values of 17.5 and 13.6 for fits to the temperature and flux curves (see dotted line in Fig. 3). The cooling curves require an exponential decay which levels off to a constant of the form $y(t) = a \exp[-(t - t_0)/b] + c$. When fitting to the data, t_0 was fixed to midday on the last day that the source was observed to be active, MJD 521 59.5. The best-fitting cooling curves are shown in Fig. 3. For the $T_{\rm eff}^{\infty}$ curve $a = 75.0 \pm 2.8$ eV, $b = 505 \pm 59$ d and $c = 51.6 \pm 1.4$ eV, with $\chi^2_{\nu} = 0.5$. For the $F_{\rm bol}$ curve $a = (4.5 \pm 0.2) \times 10^{-13}$ erg cm^{-2} s^{-1}, $b = 242 \pm 13$ d and $c = (1.7 \pm 0.3) \times 10^{-14}$ erg cm^{-2} s^{-1}, with $\chi^2_{\nu} = 0.5$.

3 DISCUSSION

We have presented *Chandra* and *XMM–Newton* observations monitoring two quasi-persistent neutron star X-ray transients (KS 1731−260 and MXB 1659−29) in a quiescent state. The long accretion episodes on to both of these neutron stars before they went into quiescence significantly heated the neutron star crust out of equilibrium with the core. The monitoring observations cover a pe-

riod of ∼4 yr since the sources returned to quiescence. Spectral fitting with an absorbed neutron star hydrogen atmosphere model to the data has clearly shown both of them cooling exponentially overtime. From the initial results of this monitoring (Wijnands et al. 2002a, 2004) and the preliminary results of Wijnands (2005) it was not clear whether either of the neutron star crusts had reached thermal equilibrium with the cores. However, the results of this latest monitoring indicates that KS 1731−260 and MXB 1659−29 have now reached equilibrium again and we have been able to measure the base level of the flux and effective temperature of these sources resulting from the state of the hot core. The additional data in this work provides a significant improvement on the previous work with respect to constraints on the cooling curve.

KS 1731−260 initially decreased by a factor of 2 in bolometric flux over the first half a year. Over the ∼4 yr since the source went into quiescence it has decreased in flux by a factor of ∼5. It reached this level ∼2.5 yr after the end of the outburst and has remained at it since then, indicating that the crust returned to equilibrium with the core in this amount of time. This base level is set by the temperature of the core, which depends on the time-averaged mass accretion rate on to the source over thousands of years. Fitting an exponential decay with a constant offset to the data we get the equilibrium temperature to be 70.0 ± 1.6 eV, and the base bolometric flux level due to thermal emission from the core as $(9.2 \pm 0.9) \times 10^{-14}$ erg cm^{-2} s^{-1}, which corresponds to a luminosity of $(5.4 \pm 0.5) \times 10^{32}$ erg s^{-1}. The e-folding times of the exponential decay were determined to be 325 ± 101 d for the temperature cooling curve and 212 ± 60 d for the flux cooling curve.

MXB 1659−29 decreased by a factor of 4 in bolometric flux over the first year after going into quiescence, and by a factor of 24 over the ∼4 yr of monitoring. Wijnands et al. (2004) found no evidence after the first three *Chandra* observations of this source that the temperature or flux was reaching a equilibrium level set by the temperature of the core. The additional last two *Chandra* observations presented here indicate that the rate of cooling has decreased. Fitting an exponential decay with a constant offset to the data reveals that it has reached the base level which we determine to be 51.6 ± 1.4 eV for the temperature and $(1.7 \pm 0.3) \times 10^{-14}$ erg cm^{-2} s^{-1} for the bolometric flux, which corresponds to a luminosity of $(2.0 \pm 0.4) \times 10^{32}$ erg s^{-1} (assuming $d = 10$ kpc). The e-folding times of the exponential decay were determined to be 505 ± 59 d for the temperature cooling curve and 242 ± 13 d for the flux cooling curve.

Rutledge et al. (2002b) calculated detailed cooling curves for KS 1731−260 predicting the behaviour of the quiescent thermal emission from the neutron star given the source's accretion history (see their fig. 3). Their models compare how the emission could evolve for standard versus enhanced core cooling and low versus high crust thermal conductivity. These authors find that regardless of the core cooling, if the crust has a low thermal conductivity, then the crust should dominate emission over the core for ∼30 yr, after which time there is a large drop in the source luminosity. For high-conductivity crusts the time-scale for this transition is much shorter, ∼1 yr. Comparing these time-scales to the observed cooling of KS 1731−260, then, in the context of these models, the crust in this source must have a high thermal conductivity (Wijnands et al. 2002a; Wijnands 2005), suggesting that it may be made of a pure iron lattice as increasing levels of impurity lower the conductivity. Unfortunately, no detailed cooling curves have been calculated for MXB 1659−29. As the cooling is dependent on the accretion history of the source, we cannot directly compare the cooling of MXB 1659−29 with the model curves calculated for KS1731−260 by Rutledge et al. (2002b). However, in these models to see a rapid drop in flux within a few years of the source going into quiescence the crust must have a high conductivity, though there may be other physical processes in the crust that allow it to cool rapidly. In particular, we note that the Rutledge et al. (2002b) models do not include Cooper-pair neutrino emission in the crust which will change the behaviour significantly (e.g. Yakovlev, Kaminker & Levenfish 1999). See the discussion in Jonker et al. (2006) for further comment on this difference.

Once the crust has cooled, the quiescent luminosity is set by the emission from the hot core (Rutledge et al. 2002b). In the standard core cooling mechanisms the heat lost by neutrino emission is negligible and thus the heat deposited in the star is radiated as thermal emission. In the case, where enhanced core cooling is allowed, the enhanced level of neutrino emission, via the direct Urca process or Cooper-pairing, means that the vast majority of heat deposited escapes as neutrinos (Colpi et al. 2001; Ushomirsky & Rutledge 2001; Rutledge et al. 2002b; Gusakov et al. 2004). If enhanced core cooling occurs, then the quiescent luminosity set by the core temperature is significantly lower than if only standard core cooling occurs. We note that continued cooling is predicted in the Rutledge et al. (2002b) models after the crust and core are in equilibrium. However, this cooling is at a significantly slower rate.

Importantly, in both sources we have now measured the thermal equilibrium temperature, which is set by the core temperature, for the first time. The quiescent luminosity at the equilibrium level of both these sources is quite typical of the quiescent emission from other 'normal' X-ray transients (e.g. see fig. 5 in Jonker et al. 2004a) whose outbursts are not as long as those of either source and last usually for only weeks to months. For the core of KS 1731−260 and MXB 1659−29 to have a similar temperature, and hence quiescent luminosity, to the other X-ray transients then either the time-averaged mass accretion rate has to be similar to the other X-ray transients, or enhanced levels of core cooling are required. For the time-averaged mass accretion rates to be similar to other X-ray transients this would require extremely long periods of quiescence of the order of hundreds to thousands of years if the observed outbursts are typical. For MXB 1659−29 there was only a period of 21 yr between outbursts and both known outbursts lasted for several years. The long time-scale accretion history for KS 1731−260 is less clear with only one outburst having been observed, however, extremely long quiescent periods are hard to explain with disc instability models (e.g. Lasota 2001). The measurement of the equilibrium level for both these sources confirms the previous findings by (Wijnands et al. 2002a, 2004; Wijnands 2005) from initial monitoring that enhanced core cooling processes are required for these sources.

Comparing the e-folding time-scales of the two sources, we find that KS 1731−260 cools at a faster rate than MXB 1659−29 (by a factor of ∼1.5), suggesting that the heat conductivity of the crust in KS 1731−260 is greater than that in MXB 1659−29. This interesting difference is likely due to differences in the properties of the crust between the two sources. In the (Rutledge et al. 2002b) models this would mean that KS 1731−260 has less impurities in the crust compared to MXB 1659−29 as a pure iron crust has a higher conductivity than one containing heavier metals also. However, one might expect the opposite to be the case, given that KS 1731−260 was actively accreting for five times longer than MXB 1659−29.

Given that we now have accurate cooling curves for these sources, and know the equilibrium level temperature, which places limits on the long-term time-averaged mass accretion rate, theoretical models need to be fit to this data to determine how high the thermal conductivity needs to be and what levels of neutrino emissions are really needed, or any alternative properties that can account for the

rapid cooling of the crust. As more than one outburst has been observed for MXB 1659−29, and because the cooling curve is much better constrained, we suggest that this source is possibly a better object to determine accurate theoretical cooling curves for than KS 1731−260.

Although some neutron star transients do not require enhanced core cooling to explain their quiescent luminosity, for example, Aql X−1, 4U 1608−522 (Colpi et al. 2001), XTE J2123−058 (assuming the recurrence time-scale is >70 yr; Tomsick et al. 2004) and SAX J1748.8−2021 in the globular cluster NGC 6440 (Cackett et al. 2005), there are several neutron star transients in addition to KS 1731−260 and MXB 1659−29 that require either very-low time-averaged mass accretion rates or enhanced core cooling to explain their quiescent luminosity, for example, Cen X-4 (Colpi et al. 2001), X1732−304 in the globular cluster Terzan 1 (Wijnands, Heinke & Grindlay 2002b; Cackett et al. 2006), RX J170930.2−263927 (Jonker et al. 2003), SAX J1810.8−2609 (Jonker, Wijnands & van der Klis 2004b), EXO 1747−214 (Tomsick, Gelino & Kaaret 2005) and 1H 1905+000 (Jonker et al. 2006). While the quiescent luminosity of KS 1731−260 and MXB 1659−29 is comparable to many quiescent neutron star transients, it is significantly higher than the emerging group of quiescent neutron star transients that are very faint in quiescence, with quiescent luminosities of less than 10^{32} erg s^{-1}. Although these faint quiescent sources include the millisecond X-ray pulsars SAX J1808.4−3658 (Campana et al. 2002), XTE J0929−314, XTE J1751−305 (Wijnands et al. 2005b) and XTE J1807−294 (Campana et al. 2005) which may have different properties due to higher magnetic fields, there are also a number of 'normal' neutron star X-ray transients that fall into this category (SAX J1810.8−2609, XTE J2123−058, EXO 1747−214). A notable faint quiescent source is the quasi-persistent neutron star transient 1H 1905+000 as although it was seen to be in outburst for at least 11 yr in the 1970s/1980s, a recent *Chandra* observation did not detect the source in quiescence, with an upper limit of 1.8×10^{31} erg s^{-1} (0.5–10 keV; for a distance of 10 kpc; Jonker et al. 2006). Apart from KS 1731−260, MXB 1659−29 and 1H 1905+000, the only other quasi-persistent source to have gone into quiescence is X1732−304 in the globular cluster Terzan 1. Using recent *Chandra* observations of Terzan 1 Cackett et al. (2006) find that the most likely quiescent counterpart to this source has a 0.5–10 keV luminosity of 2.6×10^{32} erg s^{-1}, about 6 yr after the end of an outburst that lasted at least 12 yr. For comparison, the 0.5–10 keV luminosities of the last observations of KS 1731−260 and MXB 1659−29 are $2.8^{+0.8}_{-0.6} \times 10^{32}$ erg s^{-1} and $7.5^{+3.2}_{-2.9} \times 10^{31}$ erg s^{-1}, respectively. Therefore, KS 1731−260, MXB 1659−29 and X1732−304 all have higher quiescent luminosities than 1H 1905+000. However, 1H 1905+000 was observed much longer after the end of its outburst then any of the other three sources. While the difference in quiescent luminosity may suggest that these sources will continue to cool further over the next several decades, it is more likely due to differing long-term time-averaged mass accretion rates or neutron star properties. The differences in the properties of quiescent neutron star transients need to be explored further by additional observations to determine why some sources require enhanced core cooling and why some sources are much fainter than others. Observations of the next quasi-persistent neutron star transient sources to return to quiescence (EXO 0748−676 and GS 1826−238 are both quasi-persistent sources that are still active) will help determine whether a decline in flux and temperature to a constant level on the time-scale of years, rather than decades, is typical.

We used an absorbed neutron star atmosphere model to fit to the data. If we use simple blackbody model in the spectral fitting instead, we get similar cooling curves, yet with different temperatures due to the differences between the shapes of blackbody and neutron star atmosphere spectra. When performing the spectral fits to both sources the normalization of the neutron star atmosphere component was fixed to the distance of the sources. Unfortunately, these distances are quite uncertain, thus, if the distances are wildly different from the values that we have assumed, the temperatures and fluxes that we get from the spectral fits will be incorrect. However, if the normalization is left free when fitting, then the uncertainty in this parameter dominates the errors in the other parameters. Importantly, the time-scale of the decrease in the temperature and flux of these sources should be unchanged by a different distance, only the absolute values of the temperature and flux will change. If the sources are much closer than assumed then the temperature measured will be lower and the column density higher, and the opposite if the sources are further away, as demonstrated by Wijnands et al. (2004) who fit the first three *Chandra* observations of MXB 1659−29 assuming three different distances to the source ranging from 5 to 13 kpc.

While we have interpreted the observations of KS 1731−260 and MXB 1659−29 in terms of the crust and core cooling model there are alternative models to explain quiescent neutron star emission including residual accretion or pulsar shock emission (e.g. Campana et al. 1998a; Menou et al. 1999; Campana & Stella 2000; Menou & McClintock 2001). While these are often used to explain the power-law tail present in the spectra of some neutron star transients, residual accretion can produce soft spectra if accretion occurs on to the neutron star surface (Zampieri et al. 1995). However, while variations in the luminosity of the sources in quiescence can be explained by changes in the accretion rate or the amount of matter interacting with the magnetic field, our observations show that this would have to decrease exponentially in a smooth manner over a period of several years. Given that at the end of the outbursts of 'normal' short-duration neutron star transients they reach their quiescent states within weeks (e.g. Campana et al. 1998b; Jonker et al. 2003) and that variations in accretion rate are generally not smooth, these alternative models seem unlikely.

We note that from the initial observations of both sources it was found that a power-law component (which is often attributed to residual accretion) in addition to the neutron star atmosphere component was not required to fit the spectra (Wijnands et al. 2001a, 2002a, 2003, 2004). While it has been observed that the contribution from the power-law component compared to the thermal component increases with decreasing quiescent luminosity below $\sim 10^{33}$ erg s^{-1} (Jonker et al. 2004a,b), the statistics of the last few observations are unfortunately not good enough to check for this. However, if residual accretion is occurring during quiescence it should be on-top of the 'rock bottom' thermal emission due to deep crustal heating (Brown et al. 1998; Rutledge et al. 2002b) that we have now detected. Several neutron star transients have been observed to vary during quiescence, for example, Aql X−1, Cen X−4 and SAX J1748.8−2021 in the globular cluster NGC 6440 (Rutledge et al. 2001a,b, 2002a; Campana & Stella 2003; Campana et al. 2004; Cackett et al. 2005). This variability can be interpreted as a variable power-law component, possibly due to changes in the residual accretion rate or the amount of matter interacting with the magnetic field. Unfortunately, this idea is hard to investigate with this data due to the low number of counts in the latter spectra. However, any variability in the flux from KS 1731−260 and MXB 1659−29 over the next few years around the base set by the thermal emission from the neutron star may indicate that some residual accretion is occurring.

ACKNOWLEDGMENTS

EMC gratefully acknowledges the support of PPARC. *XMM–Newton* is an ESA science mission with instruments and contributions directly funded by ESA Member States and NASA. ASM/*RXTE* results provided by the ASM/*RXTE* teams at MIT and at the RXTE SOF and GOF at NASA's GSFC.

REFERENCES

Arnaud K. A., 1996, in Jacoby G. H., Barnes J., eds, ASP Conf. Ser. Vol. 101, Astronomical Data Analysis Software and Systems V. Astron. Soc. Pac., San Francisco, p. 17
Barret D. et al., 1992, ApJ, 394, 615
Barret D., Motch C., Predehl P., 1998, A&A, 329, 965
Brown E. F., Bildsten L., Rutledge R. E., 1998, ApJ, 504, L95
Burderi L. et al., 2002, ApJ, 574, 930
Cackett E. M. et al., 2005, ApJ, 620, 922
Cackett E. M. et al., 2006, MNRAS, 369, 407
Campana S., Stella L., 2000, ApJ, 541, 849
Campana S., Stella L., 2003, ApJ, 597, 474
Campana S., Colpi M., Mereghetti S., Stella L., Tavani M., 1998a, A&AR, 8, 279
Campana S., Stella L., Mereghetti S., Colpi M., Tavani M., Ricci D., Fiume D. D., Belloni T., 1998b, ApJ, 499, L65
Campana S. et al., 2002, ApJ, 575, L15
Campana S., Israel G. L., Stella L., Gastaldello F., Mereghetti S., 2004, ApJ, 601, 474
Campana S., Ferrari N., Stella L., Israel G. L., 2005, A&A, 434, L9
Cash W., 1979, ApJ, 228, 939
Colpi M., Geppert U., Page D., Possenti A., 2001, ApJ, 548, L175
Cominsky L. R., Wood K. S., 1984, ApJ, 283, 765
Cominsky L. R., Wood K. S., 1989, ApJ, 337, 485
Cominsky L., Ossmann W., Lewin W. H. G., 1983, ApJ, 270, 226
Doxsey R., Bradt H., Johnston M., Griffiths R., Leach R., Schwartz D., Schwarz J., Grindlay J., 1979, ApJ, 228, L67
Griffiths R., Johnston M., Bradt H., Doxsey R., Gursky H., Schwartz D., Schwarz J., 1978, IAU Circ., 3190
Gusakov M. E., Kaminker A. D., Yakovlev D. G., Gnedin O. Y., 2004, A&A, 423, 1063
in 't Zand J., Heise J., Smith M. J. S., Cocchi M., Natalucci L., Celidonio G., 1999, IAU Circ., 7138
Jonker P. G., Bassa C. G., Nelemans G., Juett A. M., Brown E. F., Chakrabarty D., 2006, MNRAS, p. 395
Jonker P. G., Méndez M., Nelemans G., Wijnands R., van der Klis M., 2003, MNRAS, 341, 823
Jonker P. G., Galloway D. K., McClintock J. E., Buxton M., Garcia M., Murray S., 2004a, MNRAS, 354, 666
Jonker P. G., Wijnands R., van der Klis M., 2004b, MNRAS, 349, 94
Kuulkers E. et al., 2002, A&A, 382, 503
Lasota J.-P., 2001, New Astron. Rev., 45, 449
Lewin W., Marshall H., Primini F., Wheaton W., Cominsky L., Jernigan G., Ossman W., 1978, IAU Circ., 3190
Lewin W. H. G., Hoffman J. A., Doty J., 1976, IAU Circ., 2994
Menou K., Esin A. A., Narayan R., Garcia M. R., Lasota J.-P., McClintock J. E., 1999, ApJ, 520, 276
Menou K., McClintock J. E., 2001, ApJ, 557, 304
Muno M. P., Chakrabarty D., Galloway D. K., Savov P., 2001, ApJ, 553, L157
Muno M. P., Fox D. W., Morgan E. H., Bildsten L., 2000, ApJ, 542, 1016
Narita T., Grindlay J. E., Barret D., 2001, ApJ, 547, 420
Oosterbroek T., Parmar A. N., Sidoli L., in't Zand J. J. M., Heise J., 2001, A&A, 376, 532
Pavlov G. G., Shibanov I. A., Zavlin V. E., 1991, MNRAS, 253, 193
Remillard R. A., McClintock J. E., 2006, A&AR, 44, in press
Rutledge R. E., Bildsten L., Brown E. F., Pavlov G. G., Zavlin V. E., 2001a, ApJ, 559, 1054
Rutledge R. E., Bildsten L., Brown E. F., Pavlov G. G., Zavlin V. E., 2001b, ApJ, 551, 921
Rutledge R. E., Bildsten L., Brown E. F., Pavlov G. G., Zavlin V. E., 2002a, ApJ, 577, 346
Rutledge R. E., Bildsten L., Brown E. F., Pavlov G. G., Zavlin V. E., Ushomirsky G., 2002b, ApJ, 580, 413
Share G. et al., 1978, IAU Circ., 3190
Sidoli L., Oosterbroek T., Parmar A. N., Lumb D., Erd C., 2001, A&A, 379, 540
Smith D. A., Morgan E. H., Bradt H., 1997, ApJ, 479, L137
Sunyaev R., 1989, IAU Circ., 4839, 1
Sunyaev R., 1990, IAU Circ., 5104, 1
Sunyaev R. et al., 1990, Sov. Astron. Lett., 16, 59
Tomsick J. A., Gelino D. M., Halpern J. P., Kaaret P., 2004, ApJ, 610, 933
Tomsick J. A., Gelino D. M., Kaaret P., 2005, ApJ, 635, 1233
Ushomirsky G., Rutledge R. E., 2001, MNRAS, 325, 1157
van Paradijs J., Verbunt F., Shafer R. A., Arnaud K. A., 1987, A&A, 182, 47
Verbunt F., 2001, A&A, 368, 137
Wachter K., Leach R., Kellogg E., 1979, ApJ, 230, 274
Wachter S., Smale A. P., Bailyn C., 2000, ApJ, 534, 367
Wijnands R., 2002, in Schlegel E. M., Vrtilek S. D., eds, ASP Conf. Ser., Vol. 262, The High Energy Universe at Sharp Focus: Chandra Science Long-duration Neutron Star X-ray Transients in Quiescence: The *Chandra* Observation of KS 1731−260. Astron Soc. Pac., San Francisco, p. 235
Wijnands R., 2004, in Tovmassian G., Sion E., eds, Rev. Mex. Astron. Astrofis. Conf. Ser. Vol. 20, Compact Binaries in the Galaxy and Beyond. UNAM, Mexico, p. 7
Wijnands R., 2005, in Wass A. P., ed., Progress in Neutron Star Research. Nova Science Publishers, Hauppauge, NY (astro-ph/0405089)
Wijnands R. A. D., van der Klis M., 1997, ApJ, 482, L65
Wijnands R., Miller J. M., Markwardt C., Lewin W. H. G., van der Klis M., 2001a, ApJ, 560, L159
Wijnands R., Strohmayer T., Franco L. M., 2001b, ApJ, 549, L71
Wijnands R., Guainazzi M., van der Klis M., Méndez M., 2002a, ApJ, 573, L45
Wijnands R., Heinke C. O., Grindlay J. E., 2002b, ApJ, 572, 1002
Wijnands R., Muno M. P., Miller J. M., Franco L. M., Strohmayer T., Galloway D., Chakrabarty D., 2002c, ApJ, 566, 1060
Wijnands R., Nowak M., Miller J. M., Homan J., Wachter S., Lewin W. H. G., 2003, ApJ, 594, 952
Wijnands R., Homan J., Miller J. M., Lewin W. H. G., 2004, ApJ, 606, L61
Wijnands R., Heinke C. O., Pooley D., Edmonds P. D., Lewin W. H. G., Grindlay J. E., Jonker P. G., Miller J. M., 2005a, ApJ, 618, 883
Wijnands R., Homan J., Heinke C. O., Miller J. M., Lewin W. H. G., 2005b, ApJ, 619, 492
Yakovlev D. G., Kaminker A. D., Levenfish K. P., 1999, A&A, 343, 650
Yamauchi S., Koyama K., 1990, PASJ, 42, L83
Zampieri L., Turolla R., Zane S., Treves A., 1995, ApJ, 439, 849
Zavlin V. E., Pavlov G. G., Shibanov Y. A., 1996, A&A, 315, 141

APPENDIX A: RELATIONSHIP BETWEEN FLUX AND TEMPERATURE COOLING TIME-SCALES

Assuming that the X-rays are due to some blackbody-type emission, then the flux, F, and temperature, T, and just simply related via

$$F = AT^4, \tag{A1}$$

where $A = (R^2/D^2)\sigma$ and R is the emitting radius, D the distance, and σ the Stefan–Boltzmann constant. We are modelling the cooling of the neutron star surface as an exponential decay to a constant level, i.e.

$$T(t) = T_\infty + T'(t), \tag{A2}$$

where T_∞ is the temperature at $t = \infty$ which we assume here to be constant, and $T'(t)$ describes the evolution of the temperature of the

neutron star crust with time, which we model as:

$$T'(t) = a \exp\left(-\frac{t - t_0}{b}\right), \quad \text{(A3)}$$

with a a normalization constant, b the e-folding time, and t_0 the start time. Combining equations (A1) and (A2), leads to

$$F(t) = AT(t)^4 = A[T_\infty + T'(t)]^4. \quad \text{(A4)}$$

At the start of the cooling, when $T_\infty \ll T\prime(t)$, then the $T'(t)^4$ term dominates, and equation (A4) becomes

$$F(t) \approx AT'(t)^4 = Aa\mathrm{e}^{-4(t-t_0)/b}. \quad \text{(A5)}$$

and there should be a factor of 4 difference between the e-folding times of F and T. This was found to be the case for the initial cooling of MXB 1659−29 (Wijnands et al. 2004). However, further on in the cooling, once $T'(t) \sim T_\infty$, then the e-folding time of F becomes a complicated function of the e-folding time of T due to the constant term. Finally, once the cooling is negligable and $T'(t) \ll T_\infty$, then obviously, $F(t) = AT_\infty^4$.

This paper has been typeset from a TEX/LATEX file prepared by the author.